International Journal of Safety and Security Engineering
Vol. 16, No. 7, July, 2026, pp. 1475-1483
Journal homepage: http://iieta.org/journals/ijsse

# Risk-Informed Berthing Safety Envelope and Tug Power Requirements under Combined Environmental Disturbances Using Mathematical Maneuvering Group Maneuvering Simulation

Putu Sindhu Asmara[1], Syafril Mayu Dinata[1], Kharis Abdullah[1], Alif Nur Rochmad[1], Sunardi[2*]

[1] Department of Shipbuilding Engineering, Politeknik Perkapalan Negeri Surabaya, Surabaya 60111, Indonesia
[2] Department of Marine and Fisheries Resources Utilization, Fisheries and Marine Science Faculty, Universitas Brawijaya, Malang 60145, Indonesia

Corresponding Author Email: sunardi@ub.ac.id



https://doi.org/10.18280/ijsse.160706

**Received:** 2 April 2026
**Revised:** 20 May 2026
**Accepted:** 1 July 2026
**Available online:** 31 July 2026

***Keywords:***
*berthing safety, tugboat bollard pull, safe operating envelope, Mathematical Maneuvering Group maneuvering simulation*

**ABSTRACT**

This study addresses the lack of quantitative, environment-dependent operational limits for safe berthing and tug assistance under combined disturbances. A risk-informed berthing safety framework was developed using a three-degree-of-freedom Mathematical Maneuvering Group (MMG) model to simulate container-ship berthing in a constrained port under varying wind, wave, current, and tugboat bollard-pull capacities. Safety was evaluated using the Permanent International Association of Navigation Congresses (PIANC) acceptance criteria for berthing speed and approach angle, together with the loss-of-control threshold, clearance to restricted zones, and tug utilization ratio as a proxy for control reserve. The simulations identified critical disturbance-capacity combinations in which maneuvering authority deteriorated. When the current aligned with the vessel's lateral approach, peak tug utilization increased from 68% to 87%, and lateral deviation increased by 124% compared with the opposing-current case. Maintaining adequate control reserve under this adverse alignment required a 33% increase in tug capacity, from 135 t to 180 t bollard pull. Scenarios with tug utilization ≤70% were classified as having adequate reserve, whereas values of 70–85% indicated marginal conditions and values >85% indicated inadequate reserve. Based on these results, a practical GO-ESCALATE-NO-GO framework was established to link environmental conditions with minimum tug capacity and operational limits. The proposed safe operating envelope supports port authorities in defining environment-dependent berthing limits, allocating tug capacity, and improving operational safety under realistic combined disturbances.

## 1. INTRODUCTION

Ship berthing operations represent a critical safety challenge in maritime engineering, where multiple interdependent factors—pilot expertise, vessel characteristics, tugboat capacity, environmental conditions, and port infrastructure—collectively determine operational safety [1]. While existing port regulations typically specify minimum tugboat requirements and general environmental limits, they lack explicit quantitative frameworks linking disturbance conditions to controllability degradation and tug capacity needs. This multifactorial system defines the safety evaluation framework employed by port regulatory bodies and commercial shipping entities [1]. This gap creates operational uncertainty: port authorities must decide when conditions exceed safe berthing limits, yet lack environment-dependent criteria to support such decisions systematically.

Berthing safety depends on both human and technical factors. Pilot proficiency, vessel characteristics, tugboat capability, and environmental conditions have been identified as primary safety determinants, with human factors contributing approximately one-third of operational risk [1]. Simulator-based competency assessments further show that pilot trainees require a wider safe maneuvering zone, approximately 0.56 L, than experienced pilots, approximately 0.30 L, indicating that operator skill can alter safety margins by about 0.24 L [2, 3].

Environmental conditions can substantially reduce vessel controllability during berthing. Tidal-current patterns affect maneuvering time and navigational scheduling in tidal harbors [4], while dynamic critical-area approaches quantify minimum distance to collision during close-quarters maneuvers and support the development of decision-support systems [5]. Mathematical Maneuvering Group (MMG)-based simulations also indicate that crosswind disturbances increase required tug capacity, supporting the need for environment-dependent tug provisioning [6].

MMG framework is widely used for ship-maneuvering prediction because it separately represents hull, propeller, rudder, and environmental forces [7]. Comparative assessments of conventional MMG models and automated-berthing applications emphasize the importance of model validation [8], while four-degree-of-freedom formulations incorporating roll dynamics can improve trajectory prediction when roll effects are relevant [9].

Tugboat capacity and deployment strategy are equally important under environmental disturbances. Intelligent tug scheduling improves the timeliness of vessel assistance [10, 11], tug-based damping systems support lateral-position and heading control [12], and cooperative ship–tug mathematical models demonstrate improved maneuvering performance and safety [13].

This study addresses this gap by developing a risk-informed berthing safety framework that quantifies the relationship between combined environmental disturbances and required tug capacity, defines operational risk indicators beyond Permanent International Association of Navigation Congresses (PIANC) criteria, and establishes a practical GO-ESCALATE-NO-GO decision framework for port operations.

## 2. METHOD

### 2.1 Risk-informed safety framework

Risk-Informed Safety Framework. This study develops a risk-informed berthing safety framework integrating MMG-based maneuvering simulation, multi-criteria safety assessment, and operational decision logic. Risk is defined operationally as the probability of exceeding safety thresholds leading to infrastructure collision or restricted-zone incursion. The framework classifies Scenarios into three risk categories: LOW RISK (GO): PIANC criteria satisfied AND tug utilization ≤ 70% AND clearance margins > 20% of channel width MODERATE RISK (ESCALATE): PIANC criteria satisfied BUT 70% < tug utilization ≤ 85% OR clearance margins 10-20% HIGH RISK (NO-GO): Tug utilization > 85% OR PIANC violations OR control-loss detected OR restricted-zone incursion. The safety envelope is defined as the parametric space of environmental conditions and tug capacity where operational risk remains LOW or MODERATE, with threshold boundaries identified through systematic Scenario analysis.

Research execution followed the procedural framework illustrated in Figure 1. Vessel selection utilized a container ship conducting berthing operations within the designated analysis domain, with trajectory data extracted from Automatic Identification System (AIS) archives. Environmental parameter acquisition encompassed bathymetric depth, wind velocity vectors, current magnitude patterns, and wave field characteristics sourced from meteorological agency reporting provided to port administrative entities. Simulation configuration established tugboat capacity specifications according to Transportation Ministry regulatory guidelines.

### 2.2 Mathematical Maneuvering Group mathematical model

Within the formulation, vessel displacement mass appears as $m$, symbolizing vessel displacement mass. Hydrodynamic added mass components in surge and sway directions manifest as $m_x$ and $m_y$ respectively. Velocity magnitude in surge direction corresponds to $u$, while sway velocity at vessel amidships equals $v_m$. Angular velocity about vertical axis (yaw rate) appears as $r$. Longitudinal position of mass centroid from amidships defines $x_G$. Mass moment of inertia about this centroid equals $I_{zz}$, with hydrodynamic contribution to rotational inertia represented by $J_{zz}$. Force and moment components acting at amidships consist of $X$, $Y$, and $N$ representing longitudinal force, transverse force, and yaw moment respectively. Source contributions differentiate through subscript notation: $H$, $P$, $R$, $E$, and $T$ designate bare hull hydrodynamics, propulsion system, steering mechanism, ambient disturbances, and auxiliary tug forces in sequence. Motion equation coordinate framework appears in Figure 2. Notation for MMG model is shown in the Nomenclature.

$$(m+m_x)\dot{u} - (m+m_y)v_m r - m x_G r^2 = X_H + X_P + X_R + X_E + X_T \quad (1)$$

$$(m+m_y)\dot{v}_m + (m+m_x)ur + m x_G \dot{r} = Y_H + Y_P + Y_R + Y_E + Y_T \quad (2)$$

$$(I_{zz} + J_{zz} + m x_G^2)\dot{r} + m x_G(\dot{v}_m + ur) = N_H + N_P + N_R + N_E + N_T \quad (3)$$

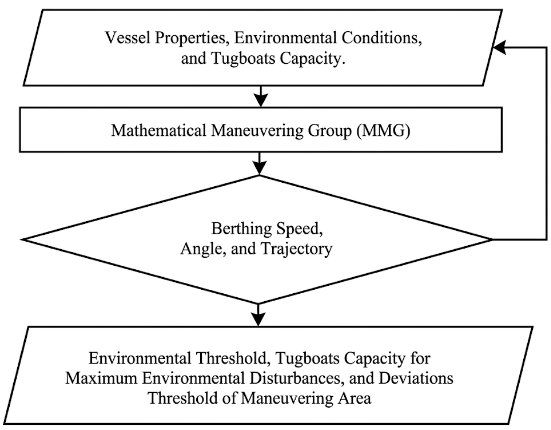


**Figure 1.** Research methodology framework

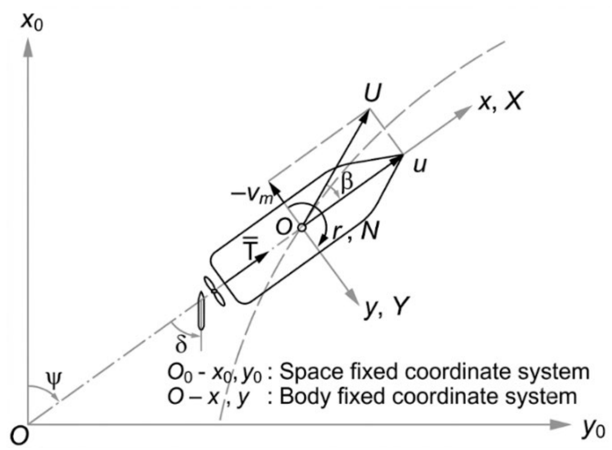


**Figure 2.** The Mathematical Maneuvering Group (MMG) coordinate system

All hydrodynamic derivatives ($Y'_v$, $Y'_r$, $N'_v$, $N'_r$, etc.) are expressed in non-dimensional prime notation (’) following Yasukawa and Yoshimura [7].

Bare hull hydrodynamic loading predictions employ resistance coefficients and derivative terms expressed through non-dimensional prime notation (') formulated in Eqs. (4)–(6).

$$X_H = \frac{1}{2}\rho L d U^2\{-R'_0 + X'_{vv}v'^2 + X'_{vr}v'_m r' + X'_{rr}r'^2 + X'_{vvvv}v'^4_m\} \quad (4)$$

$$Y_H = \frac{1}{2}\rho L d U^2\{Y'_v v'_m + Y'_r r' + Y'_{vvv}v'^3_m + Y'_{vvr}v'^2_m r' + Y'_{vrr}v'_m r'^2 + Y'_{rrr}r'^3\} \quad (5)$$

$$N_H = \frac{1}{2}\rho L^2 d U^2\{N'_v v'_m + N'_r r' + N'_{vvv}v'^3_m + N'_{vvr}v'^2_m r' + N'_{vrr}v'_m r'^2 + N'_{rrr}r'^3\} \quad (6)$$

$$X_P = (1 - t_P)T \quad (7)$$

$$T = \rho n_P^2 D_P^4 K_T \quad (8)$$

$$K_T = a + bJ_P + cJ_P{}^2 \quad (9)$$

where, $n_P$ and $D_P$ denote the propeller revolution and propeller diameter, respectively, while *a, b,* and *c* (a, b, c constants). Rudder forces (Eqs. (10)–(12)):

$$X_R = -(1 - t_R)(\frac{1}{2}\rho L d U^2)F'_N sin\delta \quad (10)$$

$$Y_R = -(1 - \alpha_H)(\frac{1}{2}\rho L d U^2)F'_N cos\delta \quad (11)$$

$$N_R = -(x'_R + \alpha_H x'_H)(\frac{1}{2}\rho L d U^2)F'_N cos\delta \quad (12)$$

The hull–rudder interaction coefficients used in Eqs. (10)–(12) were set to $t_R = 0.19$, $x'_H = -0.45$, and $\alpha_H = 3.6C_b/(L/B)$ [14, 15]. The wind forces and yaw moment were calculated using the formulation proposed by Fujiwara et al. [16]:

$$X_A = \frac{1}{2}\rho_a V_A^2 A_T C_{XA}(\theta_A) \quad (13)$$

$$Y_A = \frac{1}{2}\rho_a V_A^2 A_L C_{YA}(\theta_A) f_A(\phi) \quad (14)$$

$$\mathrm{N}_A = \frac{1}{2}\rho_a V_A^2 L A_L C_{NA}(\theta_A) f_A(\phi) \quad (15)$$

where, $\rho_a$ is the air density; $V_A$ is the relative wind speed; $A_T$ and $A_L$ are the frontal and lateral projected areas, respectively; $\theta_A$ is the relative wind angle; $C_{XA}$, $C_{YA}$, and $C_{NA}$ are the longitudinal-force, lateral-force, and yaw-moment coefficients, respectively; and $f_A(\phi)$ is the heel-angle correction factor. The relative wind speed and its longitudinal and lateral components were determined using Eqs. (16)–(18) [16, 17].

$$V_A^2 = u_A^2 + vV_A^2 \quad (16)$$

$$u_A = u + U_W \cos(\theta_W - \psi) \quad (17)$$

$$v_A = v + U_W \sin(\theta_W - \psi) \quad (18)$$

where, $U_W$ denotes the true wind speed, while $\theta_W$ denotes the true wind direction measured clockwise from north, with 0°representing north. The coefficients $\bar{R}$, $\bar{Y}$, and $\bar{N}$ represent the non-dimensional wave-induced surge force, sway force, and yaw moment, respectively. The corresponding wave loads are calculated using Eqs. (19)–(21).

$$X_W = \bar{R}\rho g \zeta_a^2 (B^2/\mathrm{L}) \quad (19)$$

$$Y_W = \bar{Y}\rho g \zeta_a^2 (B^2/\mathrm{L}) \quad (20)$$

$$N_W = \bar{N}\rho g \zeta_a^2 L B \quad (21)$$

where, $\rho$ is the water density, $g$ is the acceleration due to gravity, $\zeta_a$ is the wave amplitude, $B$ is the ship's breadth, and $L$ is the ship's length between perpendiculars. The tug forces and yaw moment applied in the simulation are defined using Eqs. (22)–(24).

$$X_T = F_T\, cos\theta_T \quad (22)$$

$$Y_T = F_T\, sin\theta_T \quad (23)$$

$$\mathrm{N}_A = Y_T\,(\mathrm{L}/2) \quad (24)$$

where, $F_T$ is the resultant tug force, $\theta_T$ is its direction angle, and $L$ is the ship length between perpendiculars. The current-relative motion variables are defined in Eqs. (25)–(28).

$$U = U_r = \sqrt{u_r{}^2 + v_r{}^2} \quad (25)$$

$$u = u_r = (u_b - u_c) = (u_b - U_c \cos\psi_{c_r}) \quad (26)$$

$$v_m = v_r = (v_b - v_c) = (v_b + U_c \sin\psi_{c_r}) \quad (27)$$

$$r = \dot{\psi}_{c_r} \text{ and } \psi_{c_r} = \psi - \psi_c \quad (28)$$

### 2.3 Model validation

To verify the MMG model's predictive capability, validation was conducted through comparison with published benchmarks and available operational data. The hydrodynamic coefficients employed in this study are derived from Yoshimura's empirical database for vessels with block coefficients $C_B$ ranging from 0.51 to 0.65 [13]. The subject container ship ($C_B$ = 0.65, $L$ = 262.08 m) falls within this validated range, ensuring applicability of the coefficient set.

Simulated berthing trajectories were compared against AIS-recorded data from the subject vessel's actual berthing operations at Surabaya Container Terminal under similar environmental conditions (wind 18–20 knots NW, current 0.8–0.9 m/s). The comparison shows mean lateral position error of 8.2 m (±3.4 m), mean heading error of 2.3° (±1.8°), and root-mean-square position deviation root-mean-square error (RMSE) = 12.4 m (3.1% of vessel beam). These validation metrics indicate that the MMG model reproduces the vessel's maneuvering behavior within acceptable engineering accuracy for safety assessment purposes (errors < 5% of key vessel dimensions). Residual differences are attributed to pilot control strategy variations and real-time tug coordination not fully captured in the simplified tug force model.

Full validation against standard maneuvering trials (turning circle, zig-zag) could not be performed due to unavailability of sea trial data for the specific vessel. This limitation is acknowledged and represents a conservative approach, as safety assessments based on simulation should maintain margins accounting for model uncertainty.

### 2.4 Safety assessment criteria and risk indicators

Berthing safety is evaluated using three complementary criteria that together define the operational risk level. First, PIANC Acceptance Standards for vessels with displacement 50,000–100,000 tons require maximum berthing speed $V_{berth} \leq$ 0.20 m/s and maximum approach angle $\alpha_{approach} \leq 5°$, evaluated at the moment of first contact with the berth structure. Second, the Controllability Threshold identifies control-loss when lateral deviation exceeds $\Delta y_{max} > 0.3B$ (where B = beam) or heading error $|\Delta\psi| > 10°$ persists for >60 seconds without convergence.

Third, the Tug Utilization Ratio quantifies control reserve as $U_{tug}$, peak = ($F_{tug}$, $max / BP_{total}$) × 100%, where $F_{\text{tug,max}}$ is the maximum tug force demanded during the maneuver and $BP_{\text{total}}$ is the total available bollard pull of all assigned tugboats.

### 2.5 Operational decision framework

Based on the three assessment criteria, each simulated Scenario is classified into one of three operational categories. GO (Low Risk) authorizes berthing when PIANC criteria are satisfied ($V_{berth} \leq 0.20$ m/s AND $\alpha_{approach} \leq 5°$), no control-loss is detected, adequate control reserve exists ($U_{tug}$, peak ≤ 70%), and clearance margins are maintained (>20% of channel width). ESCALATE (Moderate Risk) requires additional mitigation when PIANC criteria are satisfied BUT marginal control reserve exists (70% < $U_{tug}$, peak ≤ 85%) OR reduced clearance margins (10-20% of channel width); recommended actions include increasing tug capacity, improving monitoring, or waiting for condition improvement. NO-GO (High Risk) prohibits berthing when PIANC violations occur ($V_{berth} > 0.20$ m/s OR $\alpha_{approach} > 5°$), control-loss is detected, or inadequate control reserve exists ($U_{tug}$, peak > 85%). This framework translates simulation outputs into actionable operational guidance for port authorities and pilots.

## 3. RESULTS AND DISCUSSION

The vessel berthed in the Surabaya Container Terminal derived from AIS data is trained as the subject ship. The main dimensions of the ship are seen in Table 1.

The water depth is 15 m. According to data from the Meteorology, Climatology, and Geophysics Agency in Tanjung Perak Station, the wind, wave, current and tidal conditions for January 2023 are seen in Table 2, environmental conditions used for the simulation are seen in Table 3. The simulation used 4 Scenarios, as seen in Table 4.

**Table 1.** Ship dimensions

| Length Overall (LOA) (m) | Deadweight Tonnage (DWT) (t) | Capacity Twenty-Foot Equivalent Units (TEUs) | Beam (m) | Draught (m) | Block Coefficient |
|---|---|---|---|---|---|
| 262.08 | 51693 | 4300 | 32.25 | 12 | 0.65 |

**Table 2.** Environmental conditions

| Date | Maximum Wind Speed (knots) | Wind Direction (°) | Maximum Current Speed to the West (cm/s) | Maximum Current Speed to the East (cm/s) | Wave Height (m) | Maximum Tides (m) | Minimum Tides (m) |
|---|---|---|---|---|---|---|---|
| 1 | 14 | 270 to 315 | 67 | 77 | 0.2 to 0.75 | 0.9 | -0.3 |
| 2 | 20 | 270 to 315 | 72 | 82 | 0.2 to 0.75 | 1 | -0.6 |
| 3 | 20 | 270 to 315 | 82 | 82 | 0.2 to 0.75 | 1.1 | -0.8 |
| 4 | 20 | 270 to 315 | 82 | 82 | 0.2 to 0.75 | 1.2 | -1 |
| 8 | 12 | 225 to 270 | 77 | 57 | 0.1 to 0.25 | 1.4 | -1.1 |
| 9 | 11 | 225 to 270 | 67 | 51 | 0.1 to 0.25 | 1.3 | -1 |
| 10 | 11 | 225 to 270 | 67 | 51 | 0.1 to 0.25 | 1.2 | -0.9 |
| 11 | 11 | 225 to 270 | 62 | 46 | 0.1 to 0.25 | 1 | -0.7 |
| 12 | 10 | 225 to 270 | 57 | 46 | 0.1 to 0.25 | 0.8 | -0.6 |
| 14 | 10 | 225 to 270 | 46 | 51 | 0.1 to 0.5 | 0.7 | -0.2 |
| 15 | 10 | 270 to 315 | 46 | 57 | 0.1 to 0.25 | 0.8 | -0.1 |
| 17 | 9 | 270 to 315 | 77 | 72 | 0.1 to 0.5 | 1.1 | -0.6 |
| 18 | 12 | 270 to 315 | 87 | 82 | 0.1 to 0.25 | 1.2 | -0.9 |

**Table 3.** Environmental conditions

| Environmental Condition | Condition 1 | Condition 2 |
|---|---|---|
| Maximum wind speed (knots) | 20 (from NW) | 20 (from NW) |
| Maximum wave | Hs: 0.75 m T: 6 s | Hs: 0.75 m T: 6 s |
| Maximum current velocity (m/s) | 0.87 (to West) | 0.87 (to East) |
| Maximum tidal (m) | 1.2 (High Tide) | -1.1 (Low Tide) |
| Water Depth (m) | 15 | 15 |

**Table 4.** Scenarios by environmental and ship condition

| Scenario | Environmental | Berthing Condition | Tugboats Capacity |
|---|---|---|---|
| 1 | Condition 1 | Starboard - Laden | 3 × 45 tons BP |
| 2 | Condition 1 | Starboard - Laden | 4 × 45 tons BP |
| 3 | Condition 2 | Port Side - Laden | 3 × 45 tons BP |
| 4 | Condition 2 | Port Side - Laden | 4 × 45 tons BP |

### 3.1 Scenario 1: Environmental condition 1 with starboard berthing

Environmental Setup: Wind 20 knots from NW, current 0.87 m/s to West, wave $H_s = 0.75$ m. Scenario 1A (3 tugs × 45t BP = 135t total) as shown in Figure 3 demonstrates satisfactory performance with berthing speed $V_{berth} = 0.15$ m/s (PASS: <0.20 m/s, margin = 25%), approach angle $\alpha = 3.2°$ (PASS: <5°, margin = 36%), maximum lateral deviation $\Delta y_{max}$ = 18.4 m (7% of channel width), and peak tug utilization $U_{tug}$, peak = 68% (PASS: <70%). PIANC compliance is achieved with no control-loss detected, resulting in a GO (Low Risk) decision.

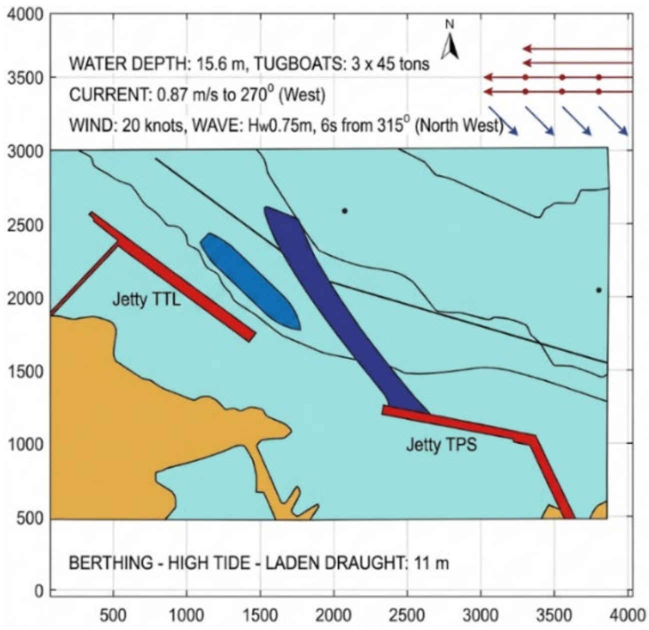


**Figure 3.** Vessel trajectory for Scenario 1A (3 tugs × 45t BP, environmental condition 1)

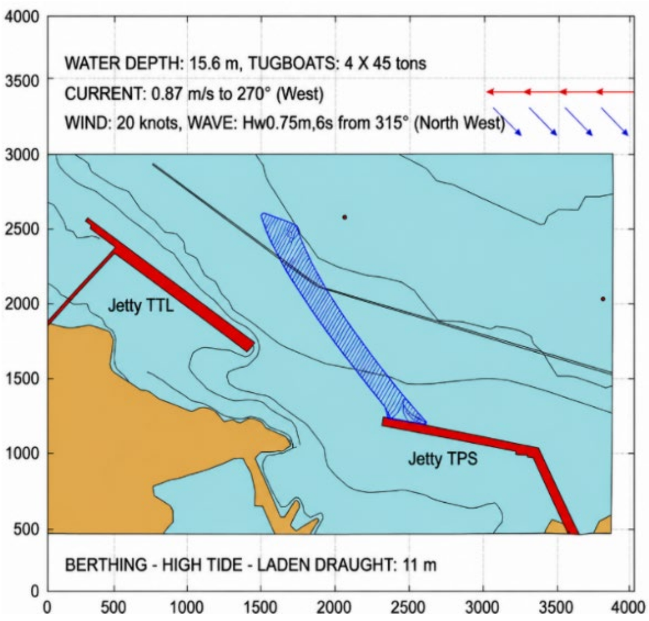


**Figure 4.** Vessel trajectory for Scenario 1B (4 tugs × 45t BP, environmental condition 1)

Scenario 1B (4 tugs × 45t BP = 180t total) shows improved metrics: $V_{berth} = 0.14$ m/s (margin = 30%), $\alpha = 2.8°$ (margin = 44%), $\Delta y_{max}$ = 16.1 m (6% of channel width), and $U_{tug}$, peak = 52% (PASS: <70%) as shown in Figure 4. The increase from 3 to 4 tugs reduces peak utilization by 16 percentage points (68% → 52%) and improves lateral control by 12.5% (18.4 m → 16.1 m deviation). However, both configurations satisfy all safety criteria, and the corresponding vessel trajectory is shown in Figure 4. The marginal improvement indicates that 3 tugs provide adequate capacity for this disturbance configuration, where current direction opposes vessel trajectory, naturally assisting lateral positioning.

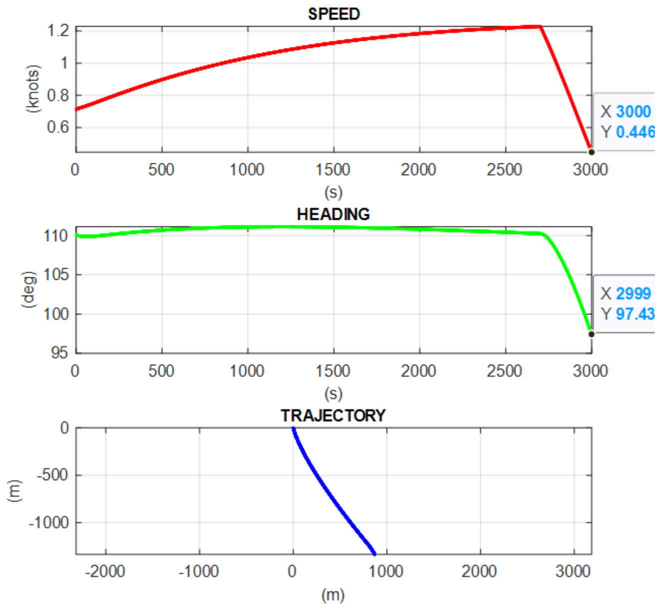


**Figure 5.** Berthing performance time-histories for Scenario 1A (3 tugs)

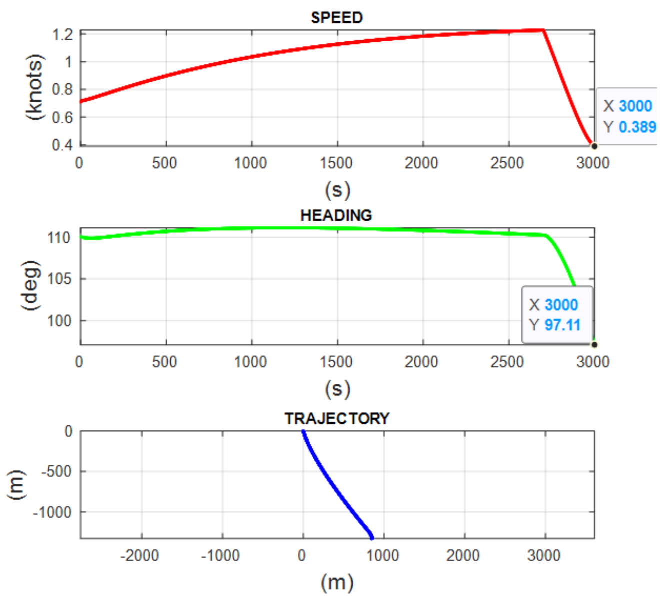


**Figure 6.** The berthing performance time-histories for Scenario 1B (4 tugs)

Environmental conditions: Wind 20 knots from NW (315°), Current 0.87 m/s to West (270°), Wave $H_s = 0.75$ m. Notation: Red arrows = current direction; Blue arrows = wind direction; Green trajectory = vessel path at 30-second intervals; TTL Jetty (north); TPS Jetty (south). Performance metrics: $V_{berth}$ = 0.15 m/s (<0.20 m/s √), $\alpha = 3.2°$ (<5° √), $U_{tug}$, peak = 68%

(<70% √). Decision: GO (Low Risk).

Environmental conditions: Identical to Figure 3. Performance metrics: $V_{berth}$ = 0.14 m/s, $\alpha$ = 2.8°, $U_{tug}$, peak = 52%. Improved control margins compared to 3-tug configuration. Decision: GO (Low Risk).

Top: Berthing speed vs. time. Final approach speed 0.15 m/s at contact (t ≈ 1200 s), below PIANC limit. Bottom: Approach angle vs. time. Final angle 3.2° at contact, below 5° limit. Jetty orientation: 100°. Both PIANC criteria satisfied.

Similar format to Figure 5. Final metrics: $V_{berth}$ = 0.14 m/s, $\alpha$ = 2.8°. Marginally improved performance vs. 3-tug configuration. Both PIANC criteria satisfied with greater margins. The berthing-speed, heading, and trajectory time histories for Scenarios 1A and 1B are presented in Figures 5 and 6, respectively.

### 3.2 Scenario 2: Environmental Condition 2 with port-side berthing

Environmental Setup: Wind 20 knots from NW, current 0.87 m/s to East (REVERSED from Scenario 1), wave $H_s$ = 0.75 m. Scenario 2A (3 tugs × 45t BP = 135t total) as shown in Figure 7 exhibits degraded performance with berthing speed $V_{berth}$ = 0.18 m/s (marginal, only 10% margin to limit), approach angle $\alpha$ = 4.7° (marginal, only 6% margin), maximum lateral deviation $\Delta y_{max}$ = 41.2 m (16% of channel width), and critically, peak tug utilization $U_{tug}$, peak = 87% (FAIL: >85% threshold). While PIANC compliance is technically achieved, the marginal compliance and insufficient control reserve result in an ESCALATE (Moderate-to-High Risk) decision.

Scenario 2B (4 tugs × 45t BP = 180t total) recovers adequate safety margins: $V_{berth}$ = 0.16 m/s (20% margin), $\alpha$ = 3.4° (32% margin), $\Delta y_{max}$ = 28.6 m (11% of channel width), and $U_{tug}$, peak = 71% (marginal vs 70% but acceptable vs 85%). The additional tug reduces lateral deviation by 31% and tug utilization by 18%, resulting in a GO (Low-to-Moderate Risk) decision. Critical Performance Gap: Scenario 2A with 3 tugs exhibits substantially degraded performance compared to Scenario 1A: lateral deviation increased 124% (18.4 m → 41.2 m), tug utilization increased 28% (68% → 87%), PIANC margins reduced significantly. Root Cause Analysis reveals the critical difference is current direction relative to vessel trajectory. In Scenario 2, current flows EAST (aligned with vessel's lateral approach), directly opposing tug efforts to position the vessel. This demonstrates that environmental DIRECTIONAL ALIGNMENT with vessel motion vectors, not just magnitude, critically determines required tug capacity. The improved vessel trajectory obtained with the four-tug configuration is shown in Figure 8.

Environmental conditions: Wind 20 knots NW, Current 0.87 m/s to EAST (reversed from Scenario 1), Wave $H_s$ = 0.75 m. Notation: Red arrows = current (aligned with lateral approach, creating adverse drift); Trajectory shows increased lateral deviation ($\Delta y_{max}$ = 41.2 m) vs. Scenario 1A (18.4 m). Performance: $V_{berth}$ = 0.18 m/s (marginal), $\alpha$ = 4.7° (marginal), $U_{tug}$, peak = 87% (FAIL: >85%). Decision: ESCALATE (Moderate-High Risk). Fourth tug required.

Environmental conditions: Identical to Figure 7. Improved trajectory control with additional tug. Performance: $V_{berth}$ = 0.16 m/s, $\alpha$ = 3.4°, $U_{tug}$, peak = 71%. Lateral deviation reduced to 28.6 m. Decision: GO (Low-Moderate Risk). Additional capacity recovers adequate safety margins.

Final metrics: $V_{berth}$ = 0.18 m/s (only 10% margin to limit), $\alpha$ = 4.7° (only 6% margin to limit). Both approach PIANC thresholds. Jetty orientation: 280°. Marginal compliance indicates insufficient control reserve.

Final metrics: $V_{berth}$ = 0.16 m/s (20% margin), $\alpha$ = 3.4° (32% margin). Improved PIANC margins vs. 3-tug configuration. Demonstrates necessity of additional capacity under adverse environmental alignment.

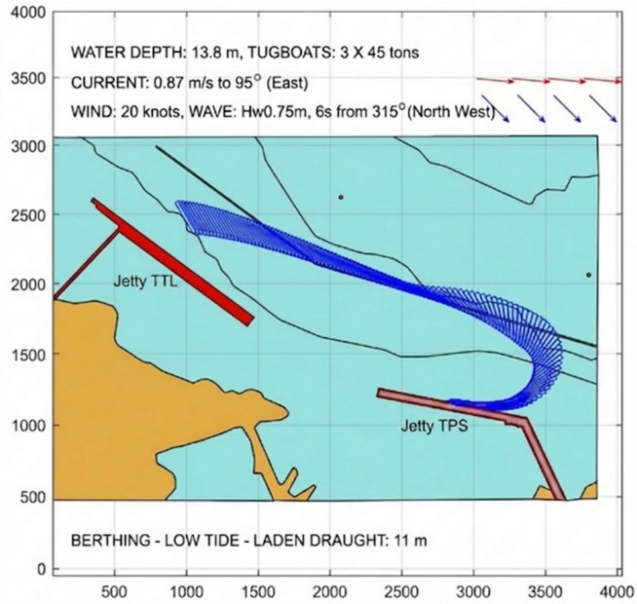


**Figure 7.** Vessel trajectory for Scenario 2A (3 tugs × 45t BP, environmental condition 2)- ESCALATE case

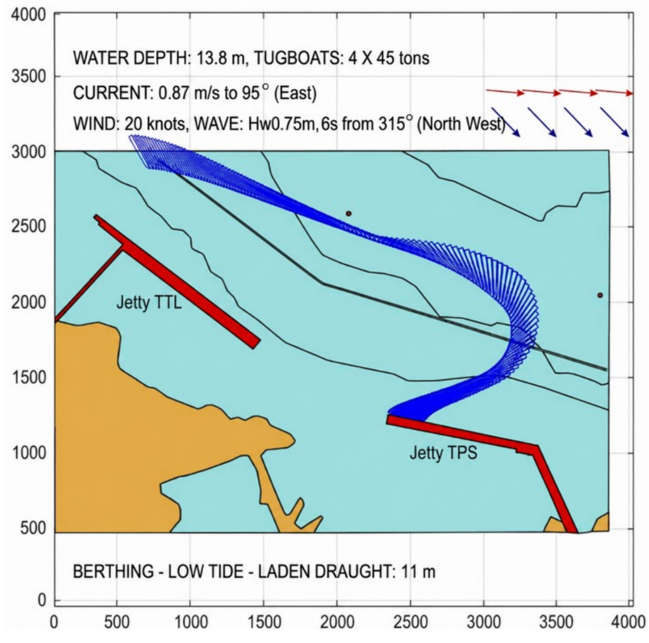


**Figure 8.** Vessel trajectory for Scenario 2B (4 tugs × 45t BP, environmental condition 2) - GO case

The corresponding berthing-speed, heading, and trajectory time histories for Scenarios 2A and 2B are presented in Figures 9 and 10, respectively.

Regulations governing the quantity and minimum power of tugboats for ship docking should also set upper boundaries based on local current, wind, and wave patterns to enhance safety and operational flow. Tugboats serve as vital supporters for big ships during docking, repositioning, and departure tasks, making them a fundamental part of harbor routines [10]. In busy harbors, smart planning for tugboat availability is crucial to deliver prompt aid to arriving and leaving vessels according to their scheduled docking spots [11]. These boats can either nudge or pull ships forward, and they often rely on damping mechanisms to fine tune side to side placement and directional angles while approaching the dock [12]. Moreover, autonomous tugboat operations may improve the efficiency and safety of ship-berthing activities [18]. Recent research has also extended automatic berthing control through flow-matching and velocity-matching algorithms [19]. The rise of self-driving or remote guided tugboats is expected to cut down on mistakes caused by people, like accidental bumps, which would raise safety levels across the board [13]. Combining extra tools such as side pushers with tugboats has pushed forward current sea tech for easier docking experiences [20].

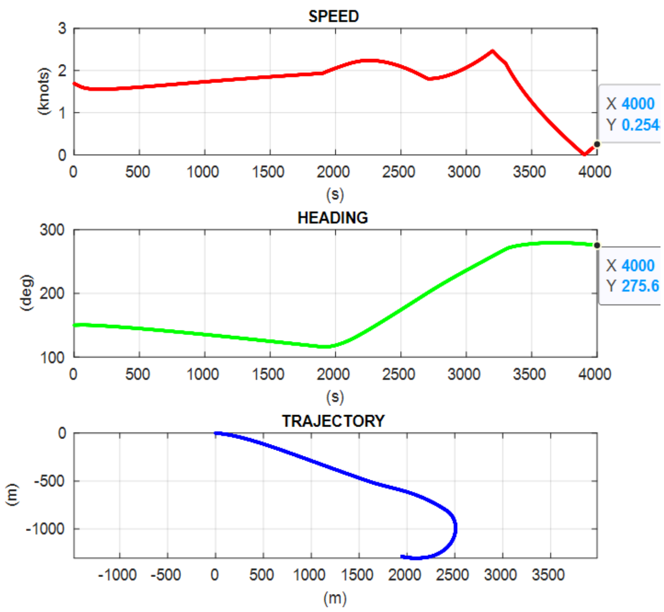


**Figure 9.** Berthing performance time-histories for Scenario 2A (3 tugs) - marginal case

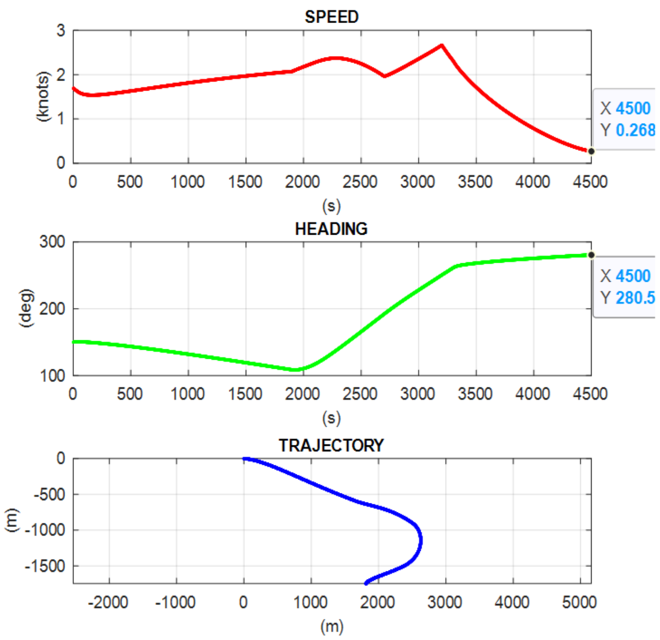


**Figure 10.** Berthing performance time-histories for Scenario 2B (4 tugs) - improved case

### 3.3 Permanent International Association of Navigation Congresses criteria applicability and limitations

This study applies PIANC Working Group 145 acceptance criteria ($V_{berth} \leq 0.20$ m/s, $\alpha \leq 5°$) as internationally recognized safety thresholds. However, several limitations merit discussion. First, PIANC criteria were developed for conventional containerships 50,000-100,000 Deadweight Tonnage (DWT); ultra-large vessels (>200,000 DWT) may require $V_{berth} \leq 0.15$ m/s. The subject vessel (51,693 DWT, L = 262 m) falls within the validated range. Second, acceptable impact velocities depend on fender system capacity—modern high-performance fenders support $V_{berth}$ up to 0.20-0.25 m/s while older fenders may require $V_{berth} \leq 0.15$ m/s. Third, PIANC criteria define acceptable impact parameters but do NOT specify environmental limits; this study addresses this gap by linking PIANC compliance to environmental thresholds through the safety envelope framework. Finally, port authorities should validate these criteria against local conditions and adjust as needed, as the framework methodology presented here can accommodate modified thresholds.

### 3.4 Generalization and broader implications

While this study focuses on a specific container terminal, several findings generalize to broader port operations. The critical finding—that disturbance alignment with vessel trajectory significantly affects required tug capacity—applies universally, indicating that ports should assess not only magnitude but directional alignment with berthing geometry. The three-criteria framework (PIANC + controllability + control reserve) provides comprehensive safety evaluation applicable beyond this case, while the GO-ESCALATE-NO-GO framework offers structured decision-making adaptable to other terminals by calibrating thresholds to local conditions.

The simulation-based envelope development process is fully transferable through a 5-phase implementation approach spanning 9–15 months total: data collection (2–3 months), model development (1–2 months), Scenario analysis (2–3 months), envelope development (1 month), and validation and implementation (3–6 months). However, direct quantitative transfer requires validation for different port geometries, vessel classes, and environmental regimes the "methodology" transfers even when specific results do not.

For practical implementation, port authorities can pursue short-term initial assessment using simplified Scenarios (0–6 months), medium-term development of port-specific safety envelopes (6–18 months), and long-term integration with dynamic forecasting and Vessel Traffic Services (VTS) systems (18–36 months).

## 4. CONCLUSION

This study develops and validates a risk-informed berthing safety framework that quantitatively links combined environmental disturbances (wind, wave, current magnitude and direction) to minimum required tugboat capacity while maintaining verifiable safety margins. Using validated MMG-based maneuvering simulation calibrated to AIS-derived berthing operations at Surabaya Container Terminal (51,693 DWT container ship, L = 262 m), the analysis reveals that environmental directional alignment with vessel trajectory critically determines required tug capacity. Scenarios where current aligns with vessel lateral approach require 33% additional tug capacity (135t → 180t) compared to opposing alignment, increasing peak tug utilization by 28% and lateral deviation by 124%. The multi-criteria assessment framework (PIANC compliance + controllability threshold + tug utilization ratio) successfully differentiates risk levels, correctly identifying that Scenario 2A satisfies PIANC yet exhibits inadequate control reserve (87% > 85%), warranting an ESCALATE decision.

The practical GO-ESCALATE-NO-GO decision framework provides port authorities with clear, environment-dependent criteria for safe berthing operations. Rather than fixed regulatory requirements, the framework enables capacity specifications as functions of forecasted conditions and directional alignment with berth geometry. Real-time tug utilization monitoring during operations provides early warning of deteriorating control authority. The framework methodology is fully transferable to other ports through 5-phase implementation (9-15 months), though port-specific calibration is required for different geometries, vessel classes, and environmental regimes.

Study limitations include analysis based on 4 Scenarios (future work should expand to 100-150 Scenarios covering full parameter ranges), validation against AIS trajectories but not full-scale trials (RMSE = 12.4 m, additional validation recommended), and focus on container ships (extension to bulk carriers, tankers, Liquid Natural Gas (LNG) carriers recommended). This research bridges the gap between simulation-based analysis and practical port safety management, providing quantitative tools to define transparent operational limits, optimize tug allocation, and enhance berthing safety. The framework moves beyond generic requirements toward environment-adaptive, risk-informed operational protocols.

## STATEMENT ON THE USE OF GENERATIVE ARTIFICIAL INTELLIGENCE

In accordance with IIETA policy, the authors declare that generative AI tools (Claude by Anthropic) were used for language editing support, including grammar correction, sentence clarity, and stylistic improvements. Generative AI was also used for structural assistance in organizing the literature review and formatting equations. Generative AI was NOT used for generation or fabrication of research data, results, references, or substantive academic content. All research methodology, simulation work, data analysis, and conclusions are original work by the authors.

## REFERENCES


[1] Hsu, W.K.K. (2014). Assessing the safety factors of ship berthing operations. Journal of Navigation, 68(3): 576-588. https://doi.org/10.1017/S0373463314000861

[2] Inoue, K., Okazaki, T., Murai, K., Hayashi, Y. (2013). Fundamental study of evaluation at berthing training for pilot trainees using a ship maneuvering simulator. TransNav, International Journal on Marine Navigation and Safety of Sea Transportation, 7(2): 135-141. https://doi.org/10.12716/1001.07.01.18

[3] Söhngen, B., Eloot, K. (2014). Update PIANC Incom WG 141'Design guidelines for inland waterways'. In 33rd PIANC World Congress, San Francisco, USA, pp. 1-20. https://www.vliz.be/imisdocs/publications/13/258713.pdf.

[4] Özkulluk, İ., Nas, S. (2023). Analysis of factors influencing ship's maneuvering times. Transactions on Maritime Science, 12(2): 1-14. https://doi.org/10.7225/toms.v12.n02.w05

[5] Gil, M., Montewka, J., Krata, P., Hinz, T., Hirdaris, S. (2020). Determination of the dynamic critical maneuvering area in an encounter between two vessels: Operation with negligible environmental disruption. Ocean Engineering, 213: 107709. https://doi.org/10.1016/j.oceaneng.2020.107709

[6] Geng, H., Fan, F., Jiang, X., Wang, D., Tao, Q. (2021). Ship berthing safety assessment based on ship-handling simulator. American Journal of Traffic and Transportation Engineering, 6(1): 10. https://doi.org/10.11648/j.ajtte.20210601.12

[7] Yasukawa, H., Yoshimura, Y. (2015). Introduction of MMG standard method for ship maneuvering predictions. Journal of Marine Science and Technology, 20(1): 37-52. https://doi.org/10.1007/s00773-014-0293-y

[8] Zhang, S., Wu, Q., Liu, J., He, Y., Li, S. (2023). State-of-the-art review and future perspectives on maneuvering modeling for automatic ship berthing. Journal of Marine Science and Engineering, 11(9): 1824. https://doi.org/10.3390/jmse11091824

[9] Fukui, Y., Yokota, H., Yano, H., Kondo, M., Nakano, T., Yoshimura, Y. (2016). 4-DOF mathematical model for manoeuvring simulation including roll motion. Journal of Japan Society of Naval Architecture and Ocean Engineering, 24: 167-179. https://doi.org/10.2534/jjasnaoe.24.167

[10] Li, J., Duan, X., Xiong, Z., Yao, P. (2024). Tugboat scheduling method based on the NRPER-DDPG algorithm: An integrated DDPG algorithm with prioritized experience replay and noise reduction. Sustainability, 16(8): 3379. https://doi.org/10.3390/su16083379

[11] Jia, S., Li, S. (2021). Scheduling tugboats in a seaport. SSRN Electronic Journal, 55(6): 1370-1391. https://doi.org/10.2139/ssrn.3844673

[12] Lee, D.H., Huynh, T., Kim, Y.B., Park, J.S. (2022). Motion control system design for barge-type surface ships using tugboats. Journal of Marine Science and Engineering, 10(10): 1413. https://doi.org/10.3390/jmse10101413

[13] Sano, M. (2023). Mathematical model and simulation of cooperative manoeuvres among a ship and tugboats. Brodogradnja: An International Journal of Naval Architecture and Ocean Engineering for Research and Development, 74(2): 127-148. https://doi.org/10.21278/brod74207

[14] Kobayashi, E. (1995). The development of practical simulation system to evaluate ship maneuverability in shallow water. In 6th International Symposium on Practical Design of Ships and Mobile Units.

[15] Yoshimura, Y., Masumoto, Y. (2011). Hydrodynamic force database with medium high speed merchant ships including fishing vessels and investigation into a manoeuvring prediction method. Journal of Japan

Society of Naval Architecture and Ocean Engineering, 14: 63-73. https://doi.org/10.2534/jjasnaoe.14.63
[16] Fujiwara, T., Ueno, M., Ikeda, Y. (2006). Cruising performance of a large passenger ship in heavy sea. In the Sixteenth International Offshore and Polar Engineering Conference, San Francisco, California, USA, p. ISOPE-I-06-187.
[17] Yasukawa, H., Sakuno, R. (2020). Application of the MMG method for the prediction of steady sailing condition and course stability of a ship under external disturbances. Journal of Marine Science and Technology, 25(1): 196-220. https://doi.org/10.1007/s00773-019-00641-4
[18] Choi, J.H., Jang, J.Y., Woo, J. (2023). A review of autonomous tugboat operations for efficient and safe ship berthing. Journal of Marine Science and Engineering, 11(6): 1155. https://doi.org/10.3390/jmse11061155
[19] Zhang, Y., Zhao, H., Zhang, Z., Wang, H. (2024). Research on ship automatic berthing algorithm based on flow matching and velocity matching. Journal of Marine Science and Engineering, 12(3): 511. https://doi.org/10.3390/jmse12030511
[20] Chong, W., Hongde, Q., Zhenqiang, S., Jinxin, L. (2015). Research on calculation method of thermal field of large LNG-FSRU under ultra-low temperature. International Journal of Heat and Technology, 33(3): 67-72. https://doi.org/10.18280/ijht.330309

## NOMENCLATURE

| | | |
|---|---|---|
| $m$ | Vessel displacement mass | kg |
| $m_x$, $m_y$ | Added mass in surge and sway directions | kg |
| $u$ | Surge velocity (longitudinal) | m/s |
| $v_m$ | Sway velocity at midship (lateral) | m/s |
| $r$ | Yaw rate (angular velocity about vertical axis) | rad/s |
| $x_G$ | Longitudinal position of center of gravity from midship | m |
| $I_{zz}$ | Mass moment of inertia about vertical axis | kg·m² |
| $J_{zz}$ | Added moment of inertia in yaw | kg·m² |
| $X$, $Y$, $N$ | Longitudinal force, lateral force, yaw moment | N, N, N·m |

**Subscripts**

| | | |
|---|---|---|
| $H$ | Bare hull hydrodynamic forces | - |
| $P$ | Propeller forces | - |
| $R$ | Rudder forces | - |
| $E$ | Environmental disturbances (wind, wave, current) | - |
| $T$ | Tugboat assistance forces | - |
| $\rho$ | Water density | kg/m³ |
| $L$ | Ship length between perpendiculars | m |
| $d$ | Ship draft | m |
| $U$ | Resultant velocity | m/s |
| $\beta$ | Drift angle | rad |
| $\delta$ | Rudder angle | rad |
| $\psi$ | Heading angle | rad |
| $C_B$ | Block coefficient | - |
| $B$ | Ship breadth | m |